J Solid State Electrochem (2012) 16:3467–3472
DOI 10.1007/s10008-012-1838-9

ORIGINAL PAPER

Kinetics of adsorption of poly(vinylimidazole) (PVI) onto copper surfaces investigated by quartz crystal microbalance studies

Tobias Simbeck · Michael Maximilian Hammer · Stefan Thomaier · Christoph Stock · Edmund Riedl · Heiner Jakob Gores

Received: 28 April 2012 / Revised: 24 July 2012 / Accepted: 1 August 2012 / Published online: 14 August 2012

Abstract Organic corrosion inhibitors offer a huge potential of lowering product cost and manufacturing complexity in printed circuit board industry. Up to now, there is no reliable and fast method available to classify materials according to their ability to prevent copper from corrosion based on kinetic data of adsorption. We investigated the potential of the recently presented fast impedance-scanning quartz microbalance (FIS-QCM) to perform such studies. We selected poly(vinylimidazole) (PVI) that is known for its excellent ability to prevent copper from corrosion. However, kinetics and free energy of adsorption of PVI were never investigated. This paper presents the results of these studies. Reliable kinetic data were obtained, and the measurements show also the excellent frequency stability of this device that enables the detection of very small changes in resonance behaviour of the sensor quartz crystal, even below 1 Hz.

Keywords Copper corrosion · Adsorption kinetics · Quartz crystal microbalance · Corrosion inhibitors · Poly (vinylimidazole)

T. Simbeck · M. M. Hammer · S. Thomaier · E. Riedl
Workgroup "Electrochemistry and Electrolytes", Institute of Physical and Theoretical Chemistry, University of Regensburg, 93040 Regensburg, Germany

C. Stock · H. J. Gores (✉)
Institute of Physical Chemistry, Münster, Electrochemical Energy Technology (MEET), Westfälische Wilhelms-Universität (WWU) Münster,
Corrensstraße 46,
48149 Münster, Germany
e-mail: hgore_01@uni-muenster.de
URL: http://www.uni-muenster.de/MEET/team/gores.html

Introduction

The good electrical and thermal properties of copper and its alloys are well known. Therefore, copper plays a major role in electronics. Despite copper showing a good resistance towards corrosion [1, 2], it is well known that copper can be affected by corrosion. Alkaline and acidic environments or presence of chloride ions have a negative impact on copper and its alloys [3]. It is obvious that under certain conditions copper needs to be protected against corrosion otherwise its good electrical and thermal properties will deteriorate.

Many inhibitors are available that prevent copper from corrosion under the influence of a chemically aggressive environment. The inhibitors differ in their chemical nature and their functional groups [1]. There are a few inorganic inhibitors such as CrO_4^{2-} [4] in contrast to organic compounds where many materials have been studied and were suggested for their use as inhibitors. In contrast to used inorganic materials, organic compounds show less toxicity but are less stable at elevated temperatures.

The most popular organic compounds are azole-based inhibitors, such as imidazoles [5], diazoles [6] and triazoles including one of the best studied compounds: benzotriazole [7–9]. The polymer poly(vinylimidazole) (PVI) belongs also to the group of the azole-based compounds. PVI is known as an effective agent to prevent copper from corrosion especially at elevated temperatures including wet environments [10, 11].

Regarding the application of corrosion inhibiting materials for copper especially, the electronic industry such as the semiconductor industry or the printed circuit board (PCB) industry offers a couple of possibilities. Copper is widely used as a soldering substrate in PCB industry; the protection

of corrosion in this application is done with metal deposition of, e.g. tin, silver or nickel–phosphorous with a thin gold layer [12].

For cheaper applications also, organic surface protection is used mainly for utilising benzotriazolium derivatives. Due to the limited thermal stability of benzotriazolium coatings in this industry, engineers are striving to a more stable organic passivation of copper, such as PVI reported in this work [13, 14].

Also for the interconnections of semiconductor chips to the package, copper is used in combination with precious metal coatings such as silver, palladium or gold to prevent the formation of copper oxide and corrosion [15–20].

Organic corrosion inhibitors at that point offer a huge potential of lowering product costs and manufacturing complexity. Furthermore, the usage of a thin film of an organic corrosion inhibitor for copper enables the direct interconnection between two copper partners such as copper wire bonding on a copper chip metallisation [21, 22].

The usage of this simple interconnect consists of only one metal type, and this prevents any formation of intermetallic phases that are known as reliability risk. One example is the couple of gold wire interconnect to an aluminium metallisation leading to brittle intermetallic phases [23].

In addition, bonding copper to a copper substrate results in an interconnect without any interfaces because there is no limitation of miscibility between the two metallic partners. In contrast, at an interface between a copper substrate and a protecting precious metal, i.e. silver, two phases (Ag and Cu) always appear due to the miscibility limits in this system. Fast interdiffusion between the copper and the thin precious metal protection such as gold leads to a vanishing of the protection layer and to a fast formation of intermetallic phases like Au_3Cu, AuCu and $AuCu_3$ at the surface. Therefore, protection of copper corrosion with a precious metal requires additional metal layers in between to minimise the interaction between the copper and the protecting metal. One example is the usage of a layer sequence of NiP, Pd and Au for the copper with NiP acting as diffusion barrier [24, 25]. In this example, the implementation of an additional nickel–phosphorous layer further complicates the system because this layer is recrystallising within thermal manufacturing processes and releasing Ni_3P [26]. Therefore, the development of organic corrosion protection coatings for copper is one focus in electronic industry.

The first experimental results concerning the protective ability of PVI were received by Fourier transform infrared reflection measurements [10]. The work presented here aims to study the formation of PVI films with the help of the quartz crystal microbalance to receive kinetic data. Conventional electrochemical polarisation measurements for equilibrium investigations were also used.

Experimental section

Materials

N-vinylimidazole (≥99 %), azobis(isobutyronitrile) (98 %) and disodiumtetraborate (99 %) were purchased from Sigma-Aldrich. Toluene (>99 %) was purchased from Acros Organics, and methanol was purchased from Merck KGaA.

Synthesis of PVI

The used polymer agent PVI was synthesised via a radical polymerisation according to the route described elsewhere [10]. The solution of 30 g *N*-vinylimidazole and 0.26 g azobis(isobutyronitrile) in 200 mL toluene was heated to 68 °C and stirred for 2 days under nitrogen atmosphere. The colourless precipitated polymer was washed several times with small amounts of toluene and afterwards dried under vacuum (10^{-9}bar) for 4 days at room temperature [10].

Equipment

The quartz crystal microbalance studies were performed with our recently presented [27] fast impedance (FIS)-scanning quartz microbalance (QCM). QCM measurements offer several well-established methods in material science [28] useful for characterising changes related to surface morphology or roughness [29], for physics and physical chemistry [30] or for bioanalytics and life-sciences [31, 32]. The QCM itself is very flexible and can be combined with electrochemistry [33] or with spectroscopic methods such as surface plasmon resonance spectroscopy [34]. The device that was used for the studies presented in this article was mainly developed by Multerer [35] and Wudy et al. [27] and is based on a FIS technique. The region of interest comprising the resonance spectrum of the quartz, is scanned stepwise collecting the amplitude of oscillation potential. This frequency window can be passed by at a maximum resolution of 0.02 Hz enabling a very precise evaluation of the characteristic resonance frequencies. Another major advantage of this device is the superior data collection rate (about 500,000 s^{-1}) that enables the observation of fast reactions at the electrode's surface during metal deposition [36, 37] or corrosion of aluminium cathode current collectors for lithium ion batteries. [38, 39]. As copper is also a current collector for lithium ion batteries (anode), this method may also be useful for this application. Due to its high-level excitation signal output, quartzes even under heavy load caused by viscoelastic deposits, such as electropolymerised poly(aniline) [27, 40] can be forced to oscillate and measured at very high accuracy. A fast internal fitting algorithm [27] evaluates the series and parallel resonance frequencies υ_s and υ_p directly after collecting the spectrum and enables

further evaluations. We were convinced that the excellent stability of frequency of this device enables the detection of very small changes in resonance behaviour of the sensor quartz crystal, even below 1 Hz, in a very good manner. Therefore, this device was used to study adsorption, where we expected that mono-molecular films are deposited to the sensor's surface, resulting in very small changes in resonance frequency.

Experiments

Commercially available gold sputtered quartzes (6 MHz standard resonance frequency; Eller, Hammersbach) were used for investigations with the quartz crystal microbalance. Copper was electrodeposited onto gold as reported elsewhere [41–43]. The copper plated quartz crystal was mounted in a vertical orientation in an in-house built cell made of Teflon [43]. Within this setup, the front side of the quartz (Cu) is in contact with the solution in the cell (see Fig. 1). During all investigations, the solution was stirred smoothly without influencing the QCM signal. The solutions were kept at a constant temperature (298±0.05) K by a thermostat (Haake KT 33). The synthesised and dried PVI was dissolved in methanol and added in small amounts to yield different weight fractions of PVI in the cell. The selected weight fractions w are rather low, 1.3×10^{-5}, 5.0×10^{-5}, 1.5×10^{-4} and 3.3×10^{-4}.

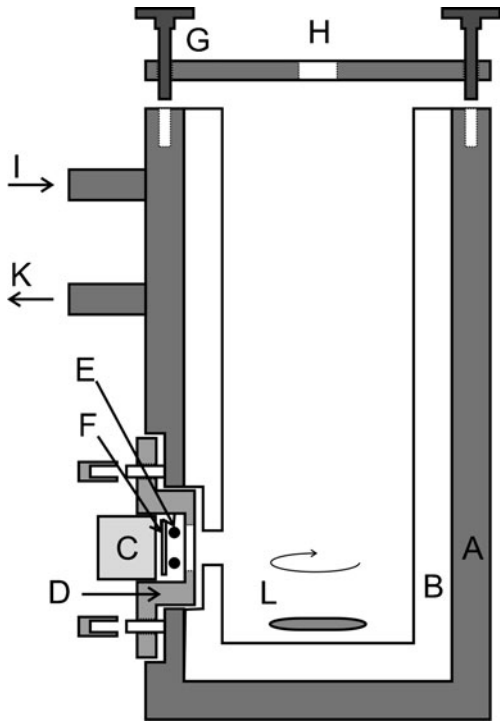

Fig. 1 Drawing of the in-house built measurement cell. *A* Aluminium jacket which is filled with the thermostatting liquid; *B* teflon measurement chamber; *C* poly(etheretherketone) screw with gold contacts for the AC signal; *D* steel device connected as ground; *E* perfluorinated rubber O-ring; *F* 0.55 in. quartz crystal; *G* aluminium top cover; *H* gas or liquid inlet; *I*, *K* temperature control liquid in- and outlet to thermostat; and *L* magnetic stirrer

For the electrochemical polarisation studies, an electrochemical workstation type IM6 of Zahner Elektrik, Kronach was used. The investigations were performed in an aqueous disodiumtetraborate buffer solution (c=0.1 molL^{-1}, pH= 10) at 298 K [44]. As working electrodes copper specimens with and without PVI coating, were used, $Ag/AgCl_{sat}$ as reference electrode and a platinum wire as counter electrode completed the setup [45]. Adsorption was performed by immersing the copper specimen in a dilute solution of PVI in methanol at the following weight fractions w of PVI in methanol: 0.01, 0.025, 0.05 and 0.1. For comparison, an uncoated specimen was electrochemically polarised as well.

Theory

The results of the QCM measurements, as well as the results of the polarisation experiments can be discussed with reference to the Langmuir model. The fundamental approach of the Langmuir isotherm is given in Eq. 1 [46].

$$\frac{d\Theta}{dt} = k_{ads}(1-\Theta)w - k_{des}\Theta \quad (1)$$

In Eq. 1, Θ represents the surface coverage of copper with PVI, t is time, k_{ads} means the kinetic adsorption constant, k_{des} the kinetic desorption constant and w the mass fraction of the inhibitor, in our case PVI. Equation 1 can be solved by yielding the following expression for the surface coverage Θ [46].

$$\Theta(t) = \frac{w}{w+\frac{k_{des}}{k_{ads}}}[1-\exp(-(k_{ads}w + k_{des})t)] \quad (2)$$

Equation 2 can be simplified by replacing $\frac{w}{w+\frac{k_{des}}{k_{ads}}}$ by a constant K_1, and also by replacing k_{obs}.

$$k_{obs} = k_{ads}w + k_{des} \quad (3)$$

The resulting Eq. 4, with the two parameters K_1 and k_{obs} can be used to fit the received quartz crystal microbalance data [46]. The fitting equation can be applied directly to the measured data, because the change in serial resonance frequency $\Delta\nu_s$ is proportional to the surface coverage Θ *(t)*.

$$\Theta(t) = K_1[1-\exp(-k_{obs}t)] \quad (4)$$

Using the linearity between w and k_{obs} (see Eq. 3), the values for k_{ads} and k_{des} are received. For the interpretation of the polarisation data, an equilibrium case is discussed. In this case, the derivation of Θ with respect

to time t (Eq. 1) is equal to zero. This leads to the following expression (Eq. 5).

$$k_{ads}(1-\Theta)w = k_{des}\Theta \tag{5}$$

Rearranging yields the Langmuir isotherm in the equilibrium case (Eq. 6)

$$\frac{\Theta}{1-\Theta} = \frac{k_{ads}}{k_{des}}w \tag{6}$$

A linear relation between $\frac{w}{\Theta}$ and w (Eq. 7) can be achieved, and again information about k_{ads} and k_{des} are available [47].

$$\frac{w}{\Theta} = \frac{k_{des}}{k_{ads}} + w \tag{7}$$

The values for the surface coverage Θ are obtained from the polarisation data, by applying the Tafel plot (Fig. 6). The received value for the current density j is used to calculate Θ (Eq. 8) [48].

$$\Theta = \frac{j_0 - j_i}{j_0} \tag{8}$$

In Eq. 8, j_0 represents the current density of an uncoated copper specimen, and j_i is the current density by coating the specimen with PVI. The kinetic approach and the equilibrium case deliver information about k_{ads} and k_{des}. Those quantities are needed to receive the free adsorption energy ΔG_{ads} by introducing the adsorption constant K (Eq. 9) [44, 46].

$$\Delta G_{ads} = -RT\ln\left(\frac{k_{ads}}{k_{des}}\right) = -RT\ln(K) \tag{9}$$

In Eq. 9, R is the universal gas constant and T is the thermodynamic temperature.

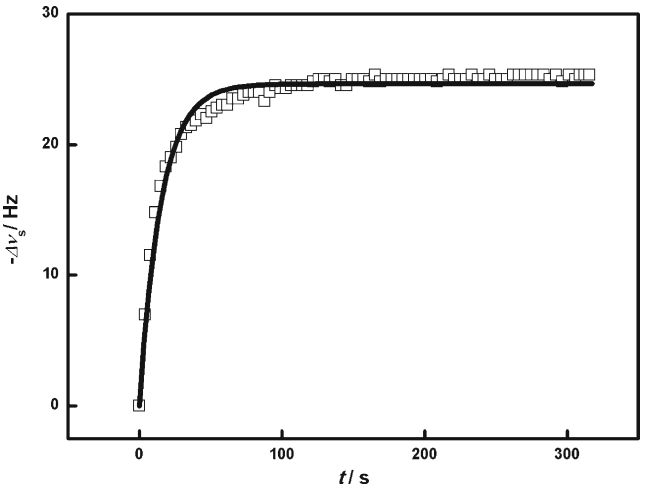

Fig. 2 QCM measurement with weight fraction $w_{PVI}=3.3\times10^{-4}$, experimental data (*squares*; only every tenth measurement is shown) and Langmuir fit (*solid line*)

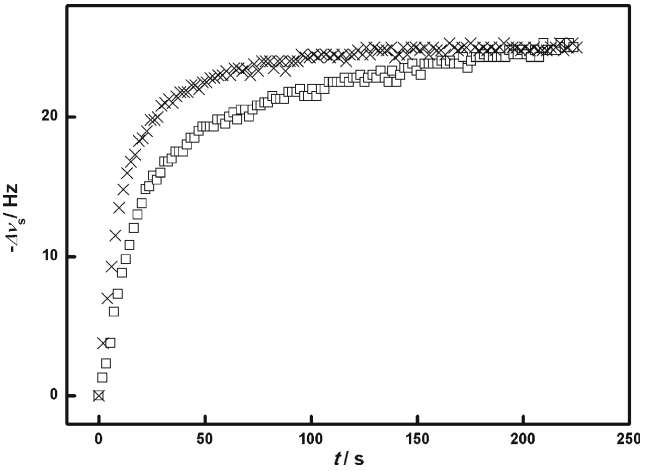

Fig. 3 QCM measurement with two different w of PVI (3.3×10^{-4} (*error marks*) and 5.0×10^{-5} (*squares*; every fifth measurement is shown for both mass fractions))

Results and discussion

FIS-QCM measurements

Frequency changes $\Delta\nu_s$ versus time t are obtained via investigations with the FIS-QCM. The frequency change $\Delta\nu_s$ is linked to a change in mass Δm at the surface of the quartz according to Sauerbrey's law [49–51] if neither the surface of the quartz is affected nor the properties of the solutions are changed. These restrictions are valid here, as only adsorption from very dilute solutions is studied. The results of the investigations (see Fig. 2) show a fast decrease in frequency with time as expected. The measurements show that the polymer adsorbs quickly onto the copper plated quartz crystal surface and thus increases the mass of the quartz by a small amount.

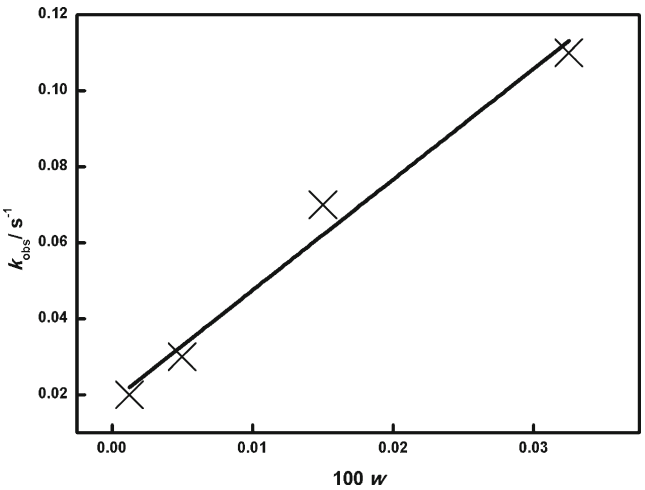

Fig. 4 Linear fit of k_{obs} vs. w (calculated results (*error marks*) and linear fit (*solid line*))

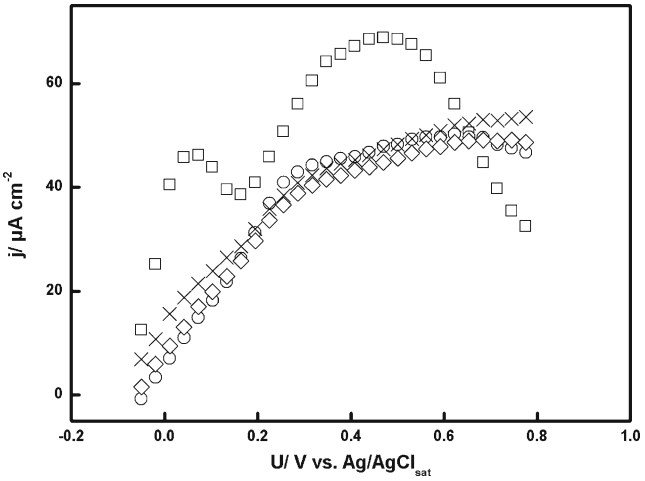

Fig. 5 Polarisation measurements with various mass fractions *w* of PVI (buffer (*squares*), 0.1 (*circles*), 0.05 (*diamonds*) and 0.01 (*error marks*); every 100th measurement is shown for all mass fractions)

In Fig. 3, different mass fractions *w* of PVI were compared. It becomes evident that the lower mass fraction takes a longer time to reach an equilibrium state than the larger one.

The kinetic effect observed by comparing two different mass fractions in their adsorption behaviour can be explained by Langmuir's isotherm model. The linear relation between k_{obs} and *w* is used (Eq. 3) to obtain the kinetic constants. The slope is proportional to k_{ads} (292 s^{-1}) and the axis intercept is proportional to k_{des} (0.018 s^{-1}) (Fig. 4).

The free adsorption energy ΔG_{ads} can be calculated from the adsorption constant *K* (Eq. 9). It is the quantity that allows comparing different species regarding their ability to be adsorbed onto copper surfaces and to prevent copper from corrosion [44, 46]. In our QCM studies, we obtained a value of −24±1 kJmol^{-1} for ΔG_{ads} including its uncertainty.

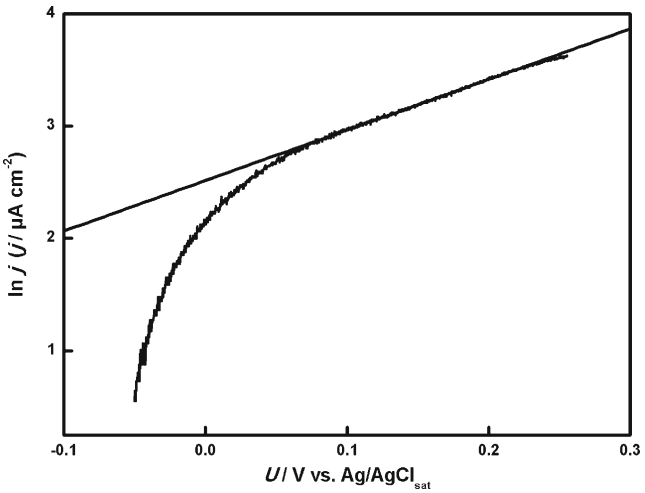

Fig. 6 Tafel plot for *w*=0.025 and linear fit

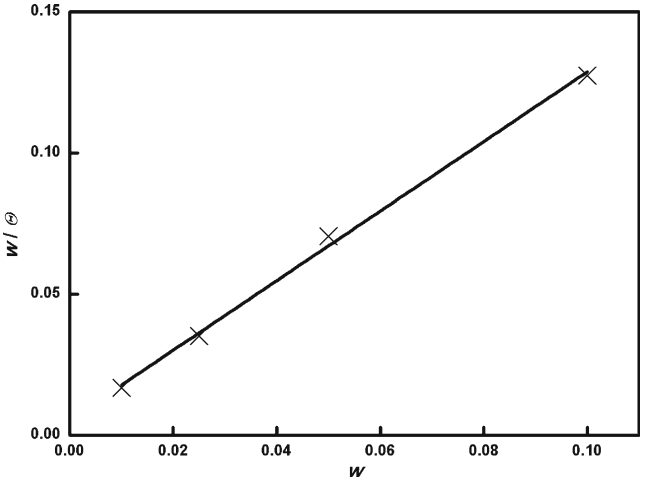

Fig. 7 Linear fit of $\frac{w}{\Theta}$ vs. *w* calculated results (*error marks*) and linear fit (*solid line*))

Polarisation measurements

In Fig. 5, three polarisation experiments are shown. To quantify the effect of PVI, again the Langmuir isotherm is applied.

As already mentioned, the Tafel plot (Fig. 6) was applied to evaluate the current densities *j* for the different mass fractions *w*.

The linear relation $\frac{w}{\Theta} = f(w)$ (see Fig. 7 and Eq. 7) yields *K*, which then was used to obtain another estimation of the free adsorption energy ΔG_{ads}.

The analysis of different mass fractions *w* of PVI leads to a free adsorption energy of −13±1 kJmol^{-1}. Weight fractions for the polarisation studies were larger than for QCM studies, but it was not possible to reach a surface coverage of nearly 100 %. Inhibition is quite independent from the weight fraction of PVI (Fig. 5). A similar effect was observed for stainless steel in acidic solution, but no value for the free adsorption energy was given there. Due to the fact that there were only two different concentrations investigated, no calculations could be done with the available data [52].

Conclusions

Currently, we check the potential of our FIS-QCM for several studies including corrosion, determination of solubility of solids in liquids, and reported in this study, corrosion inhibitors. The studies show the excellent frequency stability of this device that enables the detection of smallest changes in resonance behaviour of the sensor quartz crystal, even below 1 Hz. Measurements with the FIS-QCM show a very fast adsorption of PVI at copper. Saturation for PVI adsorption at copper is seen already after about 1 min. Polarisation measurements show a positive effect regarding corrosion inhibition, but the effect is quite independent from

the weight fraction, in agreement to the reported behaviour at stainless steel devices. In contrast, QCM measurements clearly show that different mass fractions strongly affect the adsorption behaviour. This result may also explain the largely different results for the free adsorption energy ΔG_{ads} from both methods, i.e. -24 ± 1 and -13 ± 1 kJ mol^{-1}, respectively. Kinetic constants of adsorption and desorption, respectively are $k_{ads}=292$ s^{-1} and $k_{des}=0.018$ s^{-1}.

Acknowledgements This work is dedicated to Professor Waldfried Plieth in celebration of Professor Waldfried Plieth's 75th Birthday on 7th November 2012. One of us (HJG) cordially thanks Professor Waldfried Plieth for his interest in and support of his work in several fields of electrochemistry and physical chemistry during many years. Financial support from the German Research Foundation (DFG), contract number 544243 (Project Initiative PAK 177 "Funktionsmaterialien und Materialanalytik zu Lithium-Hochleistungsbatterien") is gratefully acknowledged.

References

1. Antonijevic MM, Petrovic MB (2008) Int J Electrochem Sci 3:1–28
2. Chieb T, Belmokre K, Benmessaoud M, El Hassane Drissi S, Hajjaji N, Srhiri A (2011) Mater Sci Appl 2:1260–1267
3. Antonijevic MM, Milic SM, Serbula SM, Bogdanovic GD (2005) Electrochim Acta 50:3693–3701
4. Munoz AI, Anton JG, Guinon JL, Herranz VP (2004) Electrochim Acta 50:957–966
5. Zhang DQ, Gao LX, Zhou GD (2003) J Appl Electrochem 33:361–366
6. Lalitha A, Ramesh S, Rajeswari S (2005) Electrochim Acta 51:47–55
7. Qafsaoui W, Blanc C, Pebere N, Takenouti H, Srhiri A, Mankowski G (2002) Electrochim Acta 47:4339–4346
8. Abdullah AM, Al-Kharafi FM, Ateya BG (2006) Scripta Mater 54:1673–1677
9. Finsgar M, Milosev I (2010) Corros Sci 52:2737–2749
10. Eng FP, Ishida H (1986) J Mater Sci 21:1561–1568
11. Ishida H, Johnson R (1986) Corros Sci 26:657–667
12. Vianco PT (1999) Circ World 25:6–24
13. Eng FP, Ishida H (1986) J Appl Polym Sci 32:5021–5034
14. Xue G, Lu Y, Shi G (1994) Appl Surf Sci 74:37–41
15. Murata A, Shimada T (1990) US patent no. 4,894,752
16. Abbott D, Moehle PR (2001) US patent no. 6,194,777
17. Chang CA, Koopman NG, Roldan JM, Strickman S, Srivastava K, Yeh HL (1991) US patent no. 5,048,744
18. Takahashi S, Masukawa S, Futatsuka R, Sugimoto T, Suzuki T, Azuma C, Kanda Y, Fukatami T (1996) US patent no. 5,510,197
19. Ramsey TH, Alfaro RC (1995) US patent no. 5,455,195
20. Yang JC, Lee KC, Tan AC (1999) Proceedings of 49th electronic components and technology conference, San Diego, CA, 1–4 June, pp. 842–847
21. Whelan CM, Kinsella M, Ho HM, Maex K (2004) J Electrochem Soc 151:B33–B38
22. Ho HM, Lam W, Stoukatch S, Ratchev P, Vath CJ, Beyne E (2003) Microelectron Reliab 43:913–923
23. Breach CD, Wulff F (2004) Microelectron Reliab 44:973–981
24. Romm D, Lange B, Donald A (2001) Texas instruments application report SZZA026 July 2001. Available at: http://www.ti.com/lit/an/szza026/szza026.pdf
25. Abbott D, Romm D, Lange B (2001) Texas Instruments Application Report SZZA031 December 2001. Available at: http://www.ti.com/lit/an/szza031/szza031.pdf
26. Peeters P, Hoorn G, Daenen T, Kurowski A, Staikov G (2001) Electrochim Acta 47:161–169
27. Wudy F, Multerer M, Stock C, Schmeer G, Gores HJ (2008) Electrochim Acta 53:6568–6574
28. Song S-W, Richardson TJ, Zhuang GV, Devine TM, Evans JW (2004) Electrochim Acta 49:1483–1490
29. Bund A, Schneider M (2002) J Electrochem Soc 149:E331–E339
30. Bund A, Ispas A (2005) J Electroanal Chem 575:221–228
31. Bates RG (1976) Pure Appl Chem 45:81–97
32. Janshoff A, Steinem C (2001) Sens Update 9:313–354
33. Peipmann R, Thomas J, Bund A (2007) Electrochim Acta 52:5808–5814
34. Bund A, Baba A, Berg S, Johannsmann D, Lubben J, Wang Z, Knoll W (2003) J Phys Chem B 107:6743–6747
35. Multerer M (2007) Untersuchung an Elektrolyten für Lithium-Ionen-Zellen sowie Entwicklung und Test eines computergesteuerten, modular aufgebauten, elektochemischen Messsystems mit Quarzmikrowaage. Dissertation, Universität Regensburg
36. Lodermeyer J, Multerer M, Zistler M, Jordan S, Gores HJ, Kipferl W, Diaconu E, Sperl M, Bayreuther GJ (2006) Electrochem Soc 153:C242–C248
37. Lodermeyer J (2006) Elektrochemische Abscheidung von Metallen und Legierungen aus nichtwässrigen Systemen und Aktivierung von passivierten Metalloberflächen zur Abscheidung nanoporöser Schichten aus wässrigen Lösungen. Dissertation, Universität Regensburg
38. Moosbauer D, Zugmann S, Amereller M, Gores HJ (2010) J Chem Eng Data 55:1794–1798
39. Gores HJ, Barthel J, Zugmann S, Moosbauer D, Amereller M, Hartl R, Maurer A (2011) In: Daniel C (ed) Handbook of battery materials, Ch. 17, 2nd edn. Wiley, Weinheim, pp 525–626
40. Wudy F, Schedlbauer T, Stock C, Gores HJ (2009) Acta Chim Slov 56:65–69
41. Fonsati M, Zucchi F, Trabanelli G (1998) Electrochim Acta 44:311–322
42. Doblhofer K, Weil KG (2007) Bunsenges Mag 9:162–172
43. Simbeck T, Thomaier S, Stock C, Riedl E, Gores HJ (2011) Electrochem Commun 13:803–805
44. Milic SM, Antonijevic MM (2009) Corros Sci 51:28–34
45. Macci EM, Piatti RCV, Podesta JJ (1993) Rev Tec Ing Univ Zulia 16:101–109
46. Karpovich DS, Blanchard GJ (1994) Langmuir 10:3315–3322
47. Babic R, Metikos-Hukovic M, Loncar M (1999) Electrochim Acta 44:2413–2421
48. Tizpar A, Ghasemi Z (2006) Appl Surf Sci 252:8630–8634
49. Sauerbrey G (1959) Z Phys 155:206–222
50. Doblhofer K, Wasle S, Soares DM, Weil KG, Ertl G (2003) J Electrochem Soc 150:C657–C664
51. Hillman AR (2011) J Solid State Electrochem 15:1647–1660
52. Öncül A, Coban K, Sezer E, Senkal BF (2011) Prog Org Coat 71:167–172